

J | A | C | S

JOURNAL OF THE AMERICAN CHEMICAL SOCIETY

J. Am. Chem. Soc., 1998, 120(3), 556-563, DOI:[10.1021/ja972456v](https://doi.org/10.1021/ja972456v)

Terms & Conditions

Electronic Supporting Information files are available without a subscription to ACS Web Editions. The American Chemical Society holds a copyright ownership interest in any copyrightable Supporting Information. Files available from the ACS website may be downloaded for personal use only. Users are not otherwise permitted to reproduce, republish, redistribute, or sell any Supporting Information from the ACS website, either in whole or in part, in either machine-readable form or any other form without permission from the American Chemical Society. For permission to reproduce, republish and redistribute this material, requesters must process their own requests via the RightsLink permission system. Information about how to use the RightsLink permission system can be found at <http://pubs.acs.org/page/copyright/permissions.html>



ACS Publications

MOST TRUSTED. MOST CITED. MOST READ.

Copyright © 1998 American Chemical Society

C_{60} DIMERS: A ROUTE TO ENDOHEDRAL FULLERENE COMPOUNDS?

*Serguei Patchkovskii, Walter Thiel**

Organisch-chemisches Institut, Universität Zürich, Winterthurerstrasse 190, CH-8057 Zürich, Switzerland

SUPPORTING INFORMATION

Total energies and absolute heats of formation for the C_{60} dimer **2** and its window isomer **3**

Total energies (for *ab initio* and density functional methods) and heats of formation (for semiempirical methods) are given in Table S1.

Infrared and Raman spectra of the dimers **2** and **3**

For the analysis of the spectra, MNDO vibrational frequencies were uniformly scaled by 0.886. This scaling results in an rms deviation of 39 cm^{-1} from the experimental values^{36,74,75} for the 14 (10 Raman and 4 IR) symmetry-allowed vibrational transitions of pristine C_{60} . The resulting IR spectra for **2** and **3** are shown in Figure S1. Our program does not yet evaluate Raman intensities, so that only the frequencies of the quadrupole-allowed transitions are given in Figure S1. There is qualitative agreement between the experimental^{23-25,28,30,33,36,37,76} vibrational frequencies for various C_{60} polymers and the scaled MNDO results for dimer **2**, even though IR intensities are not well reproduced. In particular, the strong lines derived from the dipole-allowed modes of C_{60} appear at 511 cm^{-1} (exp²⁴: 526 cm^{-1}), 1155 and 1192 cm^{-1} (exp²⁴: 1183 and 1229 cm^{-1}), and 1434 and 1463 cm^{-1} (exp²⁴: 1424 and 1460 cm^{-1}). Several complex modes are also found in the $700\text{-}823\text{ cm}^{-1}$ region. Analogous modes are present in the experimental spectra²⁴, but are strongly dependent on sample preparation³⁶.

Comparison of the calculated and experimental Raman spectra for the dimer **2** is more difficult due to the lack of theoretical intensities. The easily identifiable inter-ball Raman mode appears at 87 cm^{-1} in the scaled MNDO spectrum (99 cm^{-1} unscaled), compared to 96 cm^{-1} in the experiment²⁶. The pentagonal pinch mode lies at 1463 cm^{-1} (exp⁷⁶: $1460\text{-}1464\text{ cm}^{-1}$) in dimer **2**, with a similar A_g mode appearing at 1456 cm^{-1} (exp⁷⁶: $1447\text{-}1453\text{ cm}^{-1}$).

Upon window formation, significant changes occur in the simulated spectra (see upper panel of Figure S1). The most prominent new feature in the IR spectrum corresponds to a complex vibrational mode of B_{2u} symmetry at 1562 cm^{-1} (scaled). However, five other modes of the same symmetry appear within 100 cm^{-1} in the simulated spectrum, so that both position and intensity of this mode are fairly uncertain. The pentagonal pinch mode and its satellite shift slightly in opposite directions (to 1466 and 1454 cm^{-1} , respectively). The Raman-active interball vibration shifts upwards by 6 cm^{-1} , reflecting the stiffer bridging bonds in **3**. A pair of IR- (B_{3u}) and Raman- (A_g) active modes appears in the spectra of **3** at 1700 cm^{-1} , well outside the normal range for pristine C_{60} and C_{60} polymers. Upon visual inspection, these modes can be classified as anti-phase (B_{3u}) and in-phase (A_g) vibrations of the connecting C=C double bonds, largely uncoupled from the cage motions.

Table S1. Absolute energies and heats of formation ^a for the C₆₀ dimer **2** and its window isomer **3**

	Dimer (2)	Window (3)
MNDO	1689.6	1725.3
AM1	1913.6	1949.1
PM3	1586.5	1634.2
BLYP/3-21G	-4545.50964	-4545.41120
RHF/3-21G//MNDO	-4518.00591	-4517.87680
LDA/3-21G//MNDO	-4521.19211	-4521.06099
B3LYP/3-21G//MNDO	-4547.01691	-4546.90295
BLYP/3-21G//MNDO	-4545.50276	-4545.40104
BP86/3-21G//MNDO	-4547.24310	-4547.12660
BLYP/6-311G(d)//MNDO ^b	-4571.67886	-4571.60102

^a Total energies (au) for *ab initio* and density functional methods, heats of formation (kcal/mol) for semiempirical methods. Unless noted otherwise, all density functional calculations used "SG1" numerical integration grid⁶⁸.

^b Using "Fine" numerical integration grid⁶⁸.

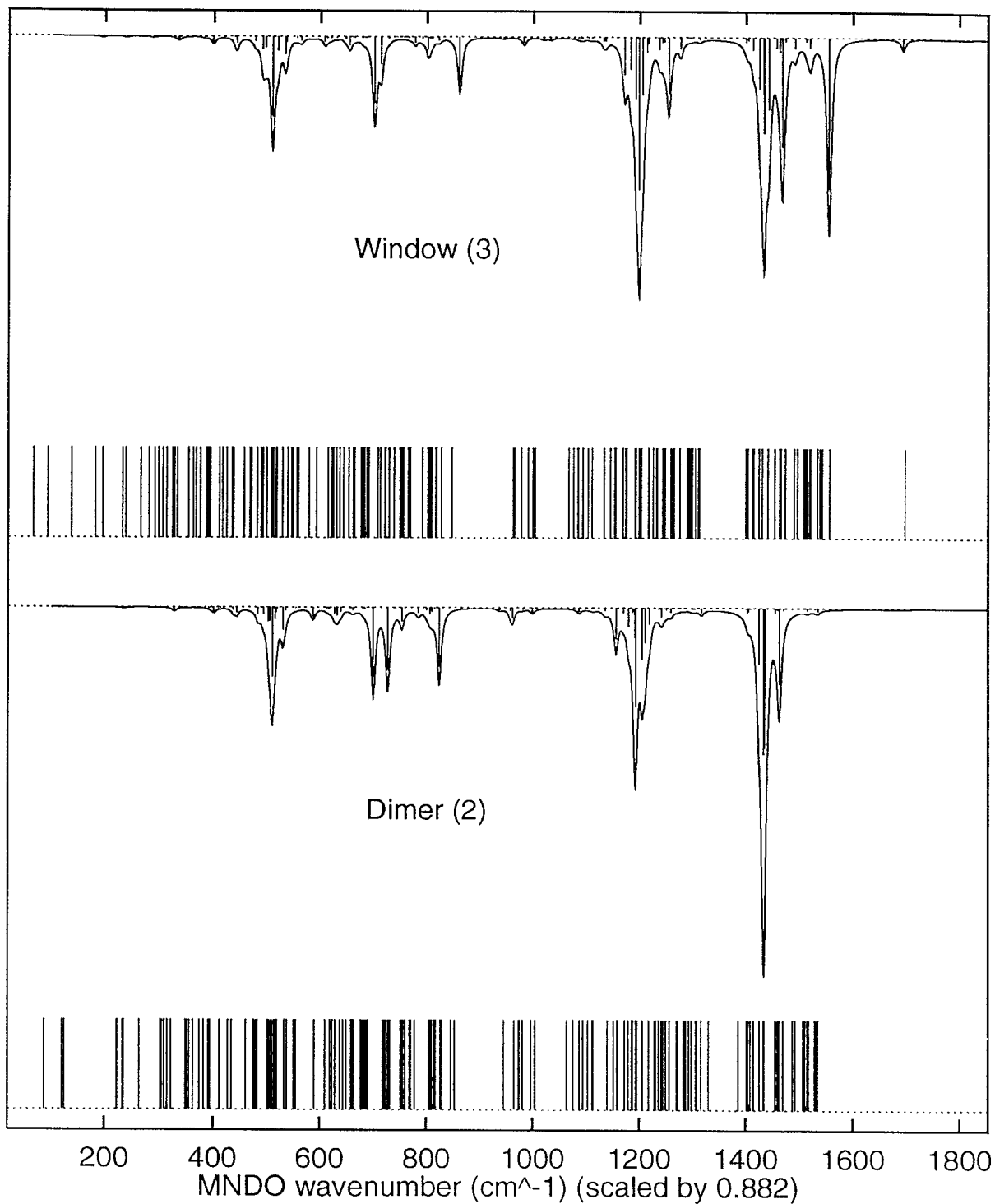


Figure S1. Calculated infrared spectra (top half of each panel) and Raman-active vibrational modes (bottom half) of the C_{60} dimer **2** and its window isomer **3**. Simulated envelopes were produced using Lorentzian line shapes with a half-width of 5 cm^{-1} .